Cancer Management and Research

Dovepress

open access to scientific and medical research

Open Access Full Text Article

ORIGINAL RESEARCH

Local Tumor Ischemia-Reperfusion Mediated By Ultrasound-Targeted Microbubble Destruction Enhances The Anti-Tumor Efficacy Of Doxorubicin Chemotherapy

This article was published in the following Dove Press journal:
Cancer Management and Research

Manxiang Wu,[1,*] Zhuqing Song,[2,*] Shiyu Zhang,[1] Qing Dan,[1] Caiyun Tang,[3] Chao Peng,[1] Yu Liang,[1] Li Zhang,[1] Hao Wang,[4] Yingjia Li[1]

[1]Department of Medicine Ultrasonics, Nanfang Hospital, Southern Medical University, Guangzhou, People's Republic of China; [2]Department of Breast Surgery, Peking University Shenzhen Hospital, Shenzhen, People's Republic of China; [3]Pharmaceutical Analysis Department, College of Pharmacy, Jiamusi University, Jiamusi, People's Republic of China; [4]Department of Neurosurgery, Shenzhen People's Hospital, The Second Clinical Medical College of Jinan University, Shenzhen, People's Republic of China

*These authors contributed equally to this work

Correspondence: Yingjia Li
Department of Medicine Ultrasonics, Nanfang Hospital, Southern Medical University, No. 1023-1063, Sha Tai Nan Road, Baiyun District, Guangzhou 510515, People's Republic of China
Tel +86 20 6164200
Email lyjia@smu.edu.cn

Hao Wang
Department of Neurosurgery, Shenzhen People's Hospital, The Second Clinical Medical College of Jinan University, No.1017 Dongmen North Road, Luohu District, Shenzhen 518020, People's Republic of China
Tel +86 755 22948200
Email hwmai@sina.com

Background: Ultrasound-targeted microbubble destruction (UTMD) has been shown to be a promising noninvasive technique to change the tumor circulation, thus providing a potential method to increase reactive oxygen species (ROS) levels in tumors by inducing tumor tissue ischemia-reperfusion (IR). In this study, we investigated the feasibility of local tumor IR through UTMD to enhance the anti-tumor efficacy of doxorubicin (DOX) chemotherapy.
Methods: UTMD was used to induce local tumor IR. After the major blood supply of the tumor was restored, DOX was intravenously injected into the tumor-bearing mice. The superoxide dismutase (SOD) and catalase (CAT) activity and ROS levels were examined, and the anti-tumor efficacy was evaluated.
Results: UTMD blocked the circulation to the tumor for 30 mins. Slow reperfusion began to occur after 30 mins, and major blood supply was restored after 1 hr. The blood perfusion of the tumor completely recovered at 2 hrs. The activity of SOD in the tumors was significantly decreased at 2 hrs and 1 day after IR treatment with or without DOX treatment. The CAT activity showed no obvious changes at 2 hrs after IR treatment, whereas a significant decrease was found after 1 day in both the IR and DOX/IR groups. Moreover, higher levels of ROS were produced in the IR group and IR/DOX group. In vivo anti-tumor study indicated that the local tumor IR strategy may significantly enhance the anti-tumor efficacy of DOX chemotherapy.
Conclusion: UTMD provides a novel, simple and non-invasive technique for tumor IR. In combination with chemotherapy, UTMD may have high great potential to improve the anti-tumor efficacy of chemotherapeutic drugs.

Keywords: ischemia-reperfusion, ultrasound targeted microbubble destruction, breast tumor, doxorubicin, combined treatment

Introduction

Combined therapy using two chemotherapeutic drugs or combining a drug chemotherapy with other treatment modalities, such as hyperthermia, photodynamic therapy, surgical operation, or radiotherapy, has become a commonly used clinical program to struggle against tumors.[1,2] Deep understanding of their mechanisms of combined therapy is essential for better antitumor efficacy. Doxorubicin (DOX) is a first-line chemotherapeutic drug for breast cancer treatment, but its antitumor efficacy is strongly affected by the levels of reactive oxygen species (ROS) in

tumors.[3] Elevated ROS levels not only may contribute to the development of cancers but also may make cancer cells more susceptible to damage induced by exogenous agents causing oxidative stress. On the other side, DOX can also enhance ROS production in cancer cells, thus resulting in oxidative stress-induced cell death.[4,5] To date, few studies have attempted to enhance the antitumor efficacy of chemotherapy agents, especially DOX, through increasing ROS production in tumors.

In recent years, many novel therapeutic strategies have been developed to improve cytotoxic ROS levels and preferentially kill cancer cells, such as the utilization of agents that can directly generate ROS or that can alternatively inhibit antioxidant enzyme systems.[6–9] More recently, ischemia-reperfusion (IR) of tumor tissue has been recognized as a promising way to induce oxidative stress. Reintroduction of oxygen to a tumor after ischemia often causes a marked increase in ROS, which can cause tumor apoptosis and necrosis.[10] The typical methods for IR are invasive and complicated procedure has to be performed. Therefore, it is desirable to develop a novel non-invasive tumor IR technique and to explore its application potential in combined chemotherapy.

Ultrasound (US) is widely used for disease diagnosis in the clinical settings, owing to its safety, ease of manipulation and low cost. Microbubbles (MBs) not only can be used as ultrasound contrast agents to monitor the tumor blood supply but also can enhance the cavitation effect of US inducing the reversible vascular effect.[11] Usually, US is used to locally deliver drugs, genes and adjuvants through ultrasound-targeted microbubble destruction (UTMD) technology.[12–16] Microbubble cavitation induced by therapeutic deliver facilitates the permeabilization of surrounding capillaries and cell membranes, thus improving cell uptake or enhanced transfection efficiency.[17] Numerous studies have demonstrated the effectiveness of UTMD in drug delivery in a number of studies. Recently, UTMD has also been demonstrated to be useful for altering the perfusion of target tissues, including temporary or permanent blockage, or improving local perfusion.[18,19] In this present study, we investigated whether UTMD might be used to generate a model of local IR in breast tumor, and we evaluated the antitumor efficacy of IR in combination with DOX chemotherapy.

Materials And Methods

Materials

The 1,2-distearoyl-sn-glycero-3-phosphatidylcholine (DSPC) and f1,2-distearoylsn-glycero-3-phosphoethanolamine-N-[methoxy(polyethyleneglycol)-2000 (DSPE-PEG2000) were purchased from Avanti Polar Lipids Inc (Alabaster, AL, USA). The LG "PRO SERIES" Ultrasound Unit was purchased from the LGMedSupply company (Cherry Hill, NJ, USA). DOX was obtained from Sigma-Aldrich (St. Louis, MO, USA). The in-situ Cell Death Detection Kit was obtained from Roche (Mannheim, Germany). CAT, SOD and ROS Kits were purchased from Jiancheng Biotechnology (Nanjing, China). The murine breast cancer 4T1 cell line was purchased from the American Type Culture Collection (Manassas, VA, USA). All other reagents were of analytical grade.

Microbubbles

MBs with a lipid-shell and perfluoropropane (C_3F_8; Flura, Newport, TN, USA) gas core were prepared as previously described.[20] Briefly, DSPC:DSPE-PEG2000 (molar ratios = 9:1) were mixed in chloroform. Then, the solvent was removed under nitrogen flow, and this was followed by vacuum treatment at room temperature to obtain a dried phospholipid film. After the dried phospholipid film was hydrated at 60°C with phosphate-buffered saline (PBS), the admixture was transferred into vials (1 mL per vial). C_3F_8 was added after the air was pumped out of the vials. Vial containing C_3F_8 and phospholipid admixture was mechanically vibrated for 30 s producing MBs.

Animal Models

Female BALB/c mice weighing approximately 20 g (6–8 weeks old) were obtained from Guangdong Medical Experimental Animal Center (Guangzhou, China). Animals received care in accordance with the Guidance Suggestions for the Care and Use of Laboratory Animals. All procedures were reviewed and approved by the ethics committee of the Southern Medical University, Chinese Academy of Sciences. To generate the breast tumor model, we subcutaneously injected 1×10^5 4T1 cells suspended in 50 μL PBS into the right flank region of the mice.

Tumor IR Models

In this study, UTMD was used to alter the local perfusion of tumors. US irradiation was begun immediately after MBs (1.25×10^8 bubbles/kg) were injected into the tail vein. Briefly, the tumor-bearing mice were irradiated with US at the tumor region for 5 mins after MBs were injected. The irradiation parameters were as follows: frequency 1 MHz, wave form pulsed, pulse repetition frequency 100 Hz, duty cycle 50%. To evaluate the blood perfusion of the tumor before and after UTMD, we performed in vivo US imaging

experiments. Briefly, after a bolus injection of 0.01 mL MBs, contrast-enhanced ultrasound (CEUS) was performed at the expected time points with a Vevo 2100 Imaging System (Visual Sonics, Canada).

Treatment Protocols

When the tumor volume reached approximately 100 mm^3, the tumor-bearing mice were randomly divided into four groups: a control group (treated with PBS), DOX group (treated with free DOX), IR group (IR induced by UTMD), and IR/DOX group (treated with DOX 1 hr after UTMD). The DOX dose was kept at 5 mg DOX per kg body weight within a final volume of 100 μL injected through the tail vein. For IR and IR/DOX groups, tumors were irradiated with US as previously described.

Activity Of Superoxide Dismutase (SOD)

A total of 24 tumor-bearing mice were randomly divided into four groups (6 mice/group), each receiving one treatment. To determine the effect of IR on ROS quenching enzymes in tumors, 3 mice of each group were sacrificed, respectively, at 1 hr and at 1 day after treatment, and the concentrations of SOD in tumors were detected with the SOD kit according to the manufacturer's instructions. In brief, oxygen produced by xanthine and xanthine oxidase forms a complex with 2-(4-iodophenyl)-3-(4-nitrophenol)-5-phenyltetrazolium chloride, which has a maximum absorbance at 550 nm. SOD activity was determined by the degree of reaction inhibition. The samples were 10 μL of 1% w/v tissues homogenate and the control samples were 10 μL of distilled water.

Activity Of Catalase (CAT)

The CAT concentration was detected at the same time point at which the SOD assay was performed. All experimental procedures followed the instructions of the manufacturer. In this method, CAT breaks down hydrogen peroxide into water and oxygen, in a manner controlled by ammonium molybdate inhibition. The residual hydrogen peroxide reacts with ammonium molybdate and forms a complex. Briefly, the control samples (5 μL of distilled water) and experimental samples (5 μL of 10% w/v tissue homogenate) were mixed with the supplied reagents, and absorbance changes at 405 nm OD were determined.

ROS Formation

ROS in tumor tissue were estimated according to the kit's instructions. Tumor samples were homogenized in ice-cold tissue culture medium. Then, samples of single cell suspension were mixed with 2,7-dichlorofluorescein diacetate (DCFH-DA). The mixture was incubated for 30 mins at 37°C. Finally, the fluorescence intensity of the samples was assessed by flow cytometry ($\lambda_{excitation}$=485 nm and $\lambda_{emission}$=525 nm).

In Vivo Anti-Tumor Evaluation

All tumor-bearing mice in the different groups (6 mice/group) received two treatments at 4-day intervals. At the end of the experimental period, all mice were sacrificed, and tumors were harvested and weighed. Throughout the experiment, tumor volumes were measured every other day.

Histological Analysis

Tumor-bearing mice were sacrificed 1 week after the last treatment by standard decapitation and the tumors and major organs (heart, liver, spleen, lung and kidney) were harvested, fixed with formalin and embedded in paraffin. Sections (5-μm) were cut with a paraffin slicing machine and stained with hematoxylin and eosin (H&E) dyes. Tumor apoptosis was also assessed by TUNEL assays which was carried out with an in-situ Cell Death Detection Kit according to the manufacturer's instructions. The ratio of cells staining positive for TUNEL in each image was determined as the ratio of the apoptotic cell number to total tumor cell number.

Statistical Analysis

Statistical analysis was carried out in SPSS software (version 19.0 for Windows; SPSS, Chicago, IL, USA). All values shown are in mean ± SD unless otherwise indicated. One-way ANOVA was used for data analysis. The differences were considered significant at $P < 0.05$, and to be very significant at $P < 0.01$.

Results

Tumor IR Models

To confirm whether the tumor IR could be achieved by US irradiation, we used CEUS to image the circulation of tumor. Figure 1A and B shows the CEUS images of the circulation of tumor before and after MBs injection□indicating that the tumor tissue had abundant blood supply. Immediately after the US irradiation (0 min point), the tumor contrast perfusion completely disappeared, and a significant perfusion defect was formed covering the targeted tumor, thus confirming that the US signals occurred

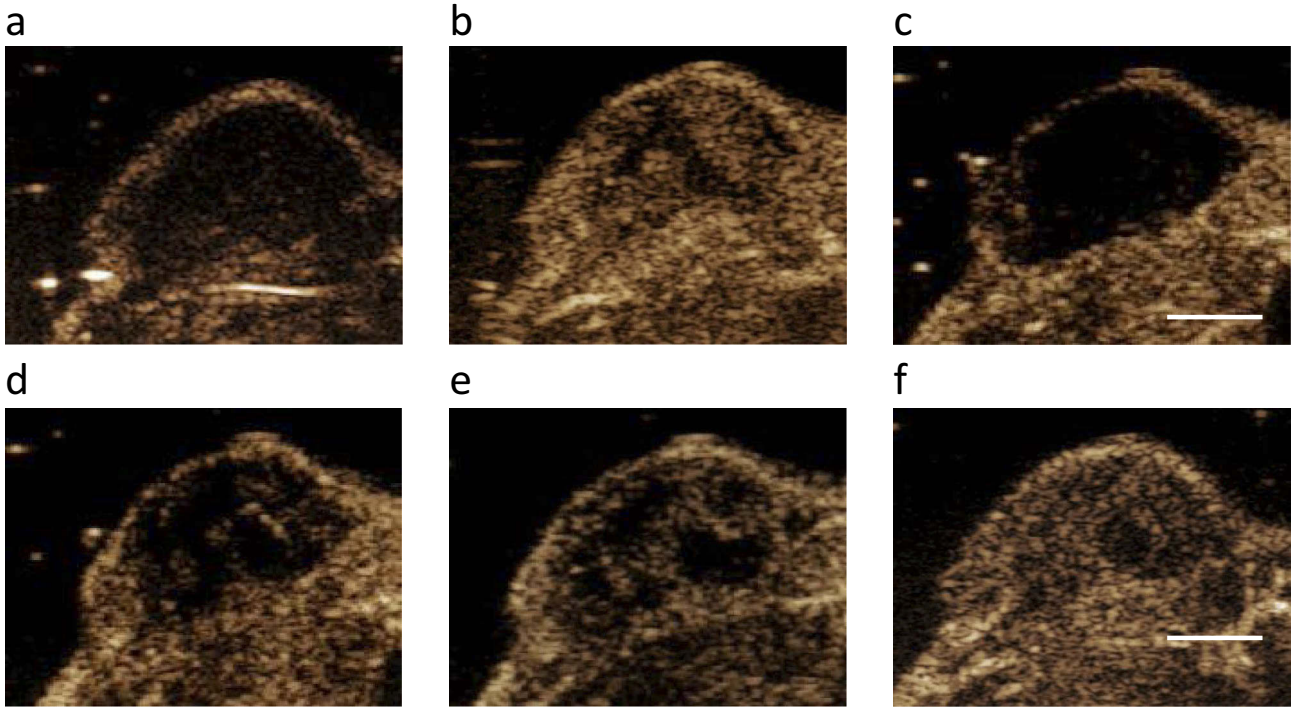

Figure 1 CEUS images of the tumor perfusion treated by US irradiation. (**A, B**) The CEUS images of a tumor before and after MBs injection. (**C**–**F**) After UTMD, a significant tumor perfusion defect occurred at 0 min (**C**), and a slow perfusion recovery occurred after 30 mins (**D**) to 1 hr (**E**). Full reperfusion was observed at 2 hrs (**F**).

at the areas enhanced with MBs (Figure 1C). After 30 mins, a small amount of perfusion recovery was observed in the tumors (Figure 1D), whereas a large amount of recovery occurred at 1 hr (Figure 1E). After 2 hrs, the blood perfusion of tumor was completely recovered (Figure 1F). These results indicated that CEUS can be used to image the tumor blood perfusion and IR in the tumor can be achieved through UTMD.

Activity Of SOD

According to the above perfusion results, the experimental group was injected with DOX at 1 hr after UTMD. Figure 2A and B shows that the activity of SOD in the control group was higher than that in the other groups at 1 hrs and 1 day after treatment. There was a slight decrease in SOD activity in DOX group at both time points, but no significant differences were observed. Interestingly, compared with the control group, the IR group and DOX+IR group showed significantly lower SOD activity at 1 hr after treatment (Figure 2A, $P<0.05$ and $P<0.001$, respectively). A further decrease in SOD activity was observed in both groups on 1 day after treatment.

Activity Of CAT

Similar results were found in the activity of CAT, another marker indicating ROS levels. The CAT activity in the DOX group was not significantly different from that in the control group at 1 hr and 1 day after treatment (Figure 3A and B). There were no significant differences between the IR group and DOX+IR group (Figure 3A) at 1 hr after treatment. In contrast, the IR group and DOX+IR group showed significantly lower CAT activity than the control group at 1 day after treatment (Figure 3B, $P<0.001$).

Production Of ROS

Tumor ROS levels in the control group were the lowest among the four groups at 1 hr and 1 day after treatment, and no significant differences were found between the control group and the DOX group (Figure 4A and B). After IR treatment, the ROS levels in the IR group and IR/DOX group showed significant increases. Moreover, the ROS levels in both groups increased over time within 1 day. Among the four groups, ROS formation in the combined treatment group (IR/DOX group) was significantly higher than that in the single treatment groups (IR group and DOX group) and the control group.

In Vivo Anti-Tumor Efficacy

The in vivo anti-tumor efficacy was further evaluated with the 4T1 subcutaneous tumor model. The IR group, compared with the control group, did not exhibit obvious tumor

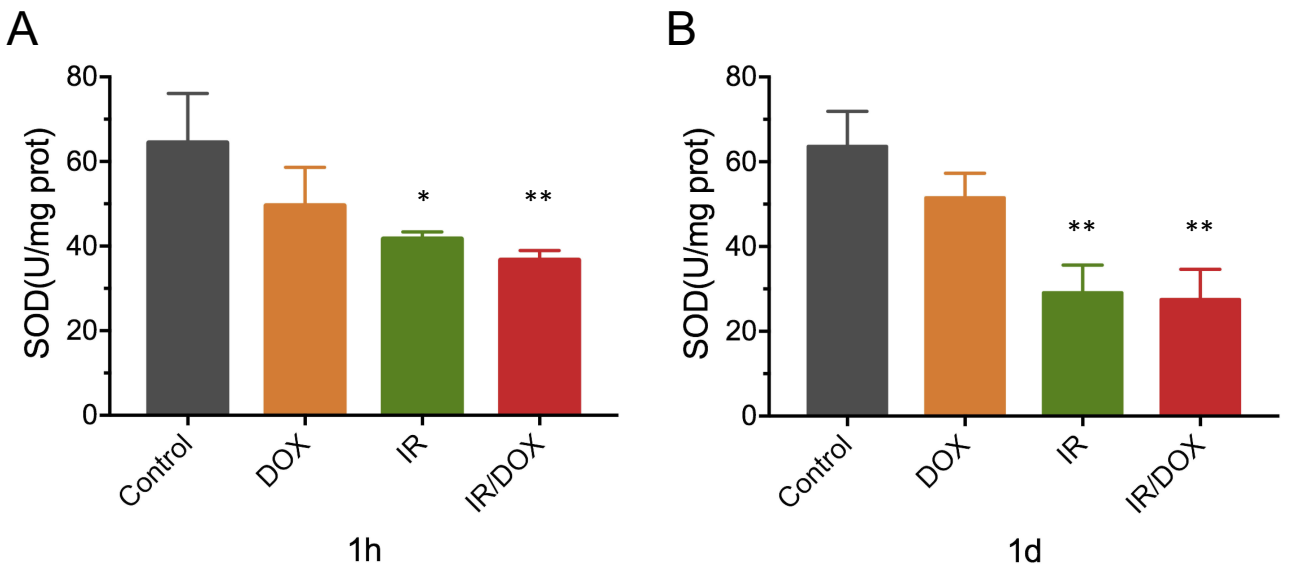

Figure 2 The activity of SOD in tumors after different treatments. The changes in SOD activity in tumors at 1 hr after treatment (**A**). The changes in SOD activity in tumors at 1 day (**B**) after different treatments. Data represented mean ± SD (n=3). Compared with controls: *P < 0.05, **P < 0.01.

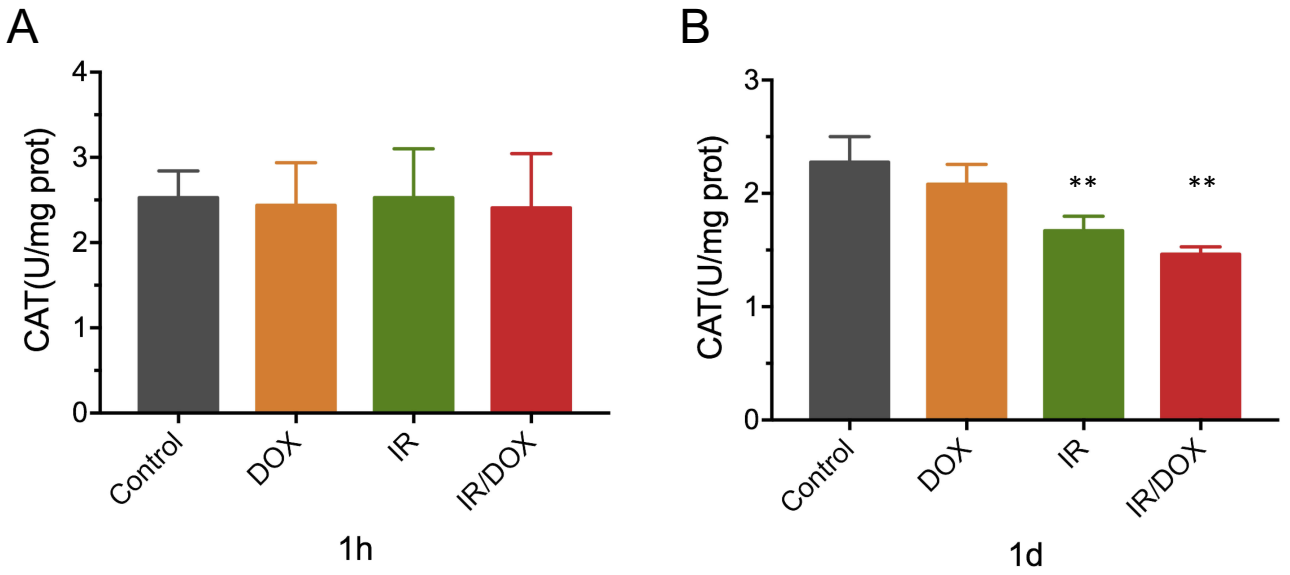

Figure 3 The activity of CAT in tumors after different treatments. The changes in CAT activity in tumors at 1 hrs after treatment (**A**). The changes in CAT activity in tumors on 1 day (**B**) after different treatments. Data represented mean ± SD (n=3). Compared with controls: **P < 0.01.

inhibition effect (Figure 5A). Moreover, the mice receiving DOX and DOX+IR, in comparison with the control treatment, showed significant tumor growth inhibition, eventually reaching a tumor volume of approximately 433.08 ± 69.47 mm^3 and 262.00 ± 54.44 $mm^{3,}$ respectively, at 15 days ($P < 0.05$). Notably, the group receiving DOX+IR treatment showed the stronger tumor growth inhibition than the other three groups. The results for tumor weight were similar to those for tumor volume (Figure 5B).

Histological Analysis

Next, histological analysis was performed with H&E and TUNEL staining. Significant tumor necrosis with severe structural damage was observed in the tumors receiving DOX+IR (Figure 6A). In comparison, tumors receiving no treatment or IR only showed only little necrosis, and tumors receiving DOX showed a small amount of necrotic cells, thus further demonstrating the treatment efficacy of DOX+IR. To further validate the tumor cell apoptosis, we analyzed the

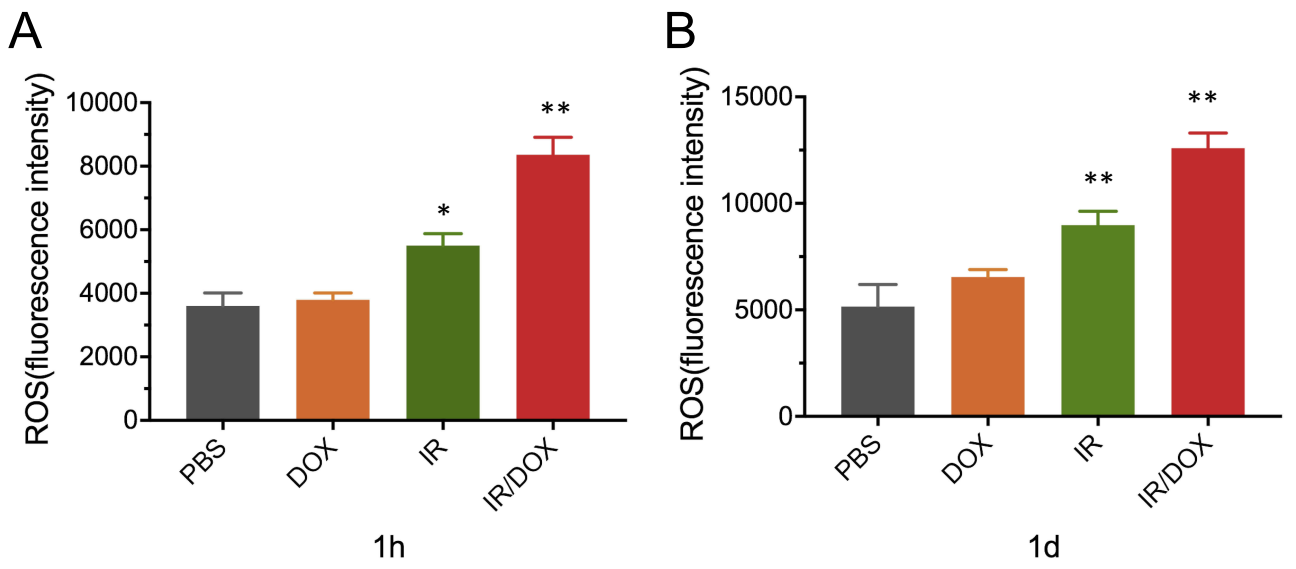

Figure 4 The production of ROS in tumors after different treatments. The fluorescence intensity of ROS in tumors at 1 hr after treatment (**A**). The fluorescence intensity of ROS in tumors on 1 day (**B**) after different treatments. Data represented mean ± SD (n=3). Compared with controls: *P < 0.05, **P < 0.01.

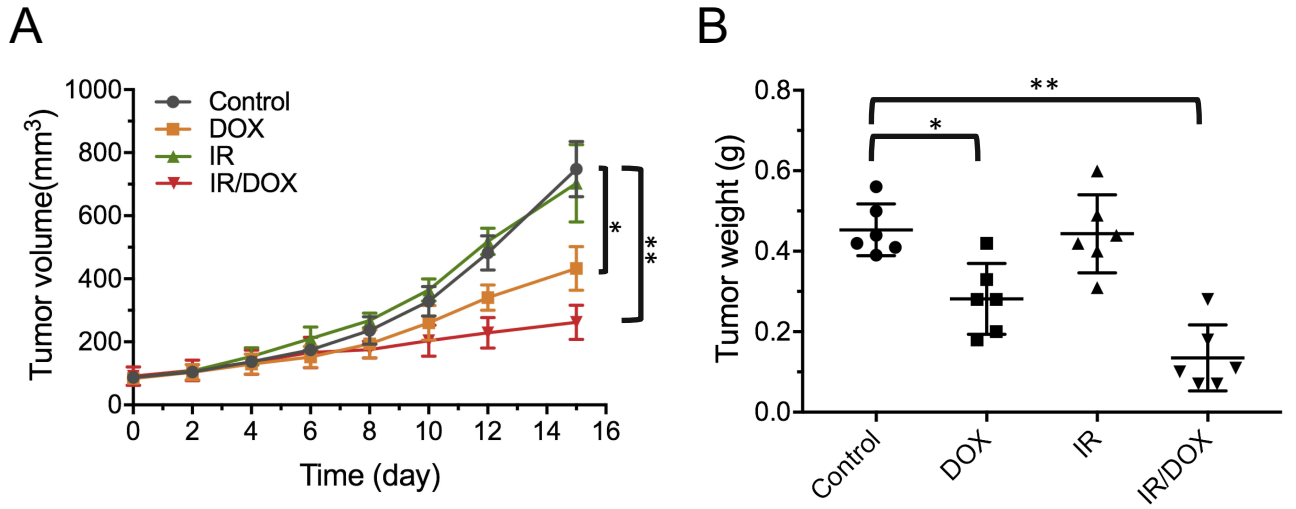

Figure 5 The in vivo anti-tumor efficacy. (**A**) The tumor growth curves during 15 days after treatment. (**B**) The weights of tumors removed from mice after 15 days of treatment. Data represented mean ± SD (n=6). Compared with controls: *P < 0.05, **P < 0.01.

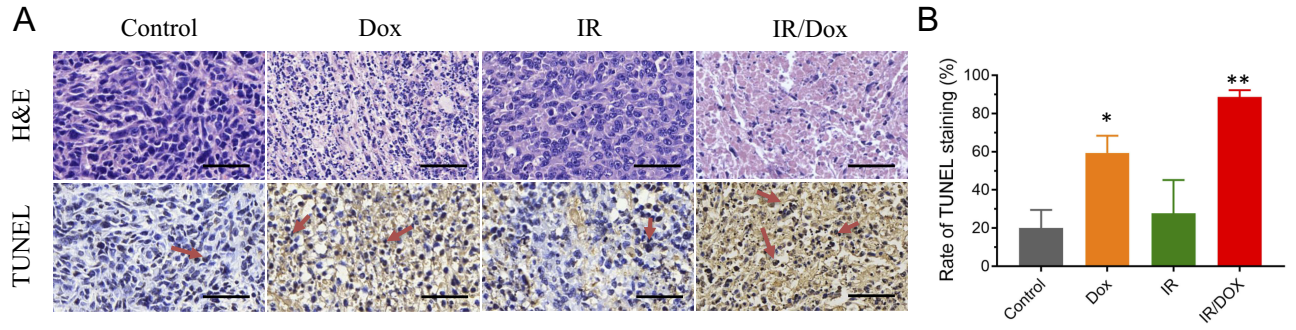

Figure 6 Histological analysis of tumors after different formulations. (**A**) H&E and TUNEL staining of tumors from mice after treatment with PBS, DOX, IR and IR/DOX (scale bar, 50 μm). (**B**) Relative rate of TUNEL staining for the different treatment groups. Data represented mean ± SD. Compared with controls: *P < 0.05, **P < 0.01.

tumor sections with a TUNEL detection kit. The relative ratio of TUNEL staining indicated that the DOX group had obvious advantages over the control group in promoting apoptosis of cancer cells ($P < 0.05$). A significant difference was observed relative to the IR+DOX group ($P < 0.001$), indicating that IR+DOX was more effective in inducing apoptosis. The above results further confirmed the presence of more apoptotic tumor cells within the tumors treated with IR+DOX (Figure 6A and B).

Discussion

US is an important tool in disease diagnosis since it has many characteristics, such as convenience, safety and real-time imaging capability. In recent decades, studies have increasingly focused on the potential role of US in the field of disease treatment, especially in cancer treatment. At present, UTMD is widely used to locally deliver drugs, genes and therapeutic cells.[21–24] More recently, many studies have found that UTMD can change the circulation of the US irradiation region.[18,19] In this study, we used the UTMD technique to induce local IR of the tumors, taking advantages of the effects of US irradiation on the blood supply in the irradiated area. The blood circulation in breast tumors was nearly blocked off at the beginning of UTMD, and this phenomenon lasted about 30 mins (Figure 1). After 1 hr, the circulation of tumor was markedly restored, especially for these larger blood vessels, and the circulation was fully restored at 2 hrs after UTMD treatment. These results may be attributed to UTMD increasing tumor vascular permeability, mild vascular injury and cell edema, thereby achieving temporary blockade of the tumor blood supply.[25] According to our experimental results, we found that the circulation blocking effect lasted about 1 hr, indicating UTMD can be used as a noninvasive and repeated method to achieve a tumor IR model.

ROS are usually regarded as injurious factors in the development of disease, and their role in anticancer effects has received increasing attention in recent years.[26–29] In our present study, US-induced tumor IR model was used to compare the effects of IR on ROS quenching enzymes in breast tumor tissues. Our data showed that the SOD activity of tumor tissues was significantly decreased at 1 hr and kept at a decreased level at 1 day in the IR and IR/DOX groups compared with the control group (Figure 2). The use of antioxidants such as SOD has been found to decrease the efficacy of anti-tumor therapies by enabling cancer cells with frequent mitochondrial DNA mutations to resist against oxidative stress, host anti-cancer surveillance, or chemotherapeutic agents.[30–32] The use of controlled IR triggered apoptosis of cancer cells has been reported previously for malignancies,[33] moreover, here we showed, that breast tumors are sensitive to apoptosis triggered by IR plus DOX. No significant differences were observed in CAT activity among the four groups at 1 hr, but the CAT activity in the IR and IR/DOX group significantly decreased at 1 day (Figure 3). CAT protects tumor cells against intercellular ROS signaling-controlled induction of apoptosis, but methods that can decrease or even inactivate CAT activity would promote intracellular ROS-mediated apoptosis.[34] In our study, the expression of CAT activity in IR tumor tissue is decreased. Thus, malignant cells produced superoxide anions that drove apoptotic signaling with high selectivity for malignant cells. In addition, ROS levels as a direct indicator of oxidative stress were significantly increased in the IR and IR/DOX group comparing with control group, and the upward trends continued in both groups, in contrast to the changes of SOD and CAT activity (Figure 4).

Since UTMD induced IR can improve ROS levels in tumor regions, and the tumor-killing effect of DOX is largely affected by the levels of ROS in tumors, the anti-tumor efficacy of the combination treatment was investigated in this study. Our data from the in vivo anti-tumor experiments clearly showed that IR plus DOX resulted in more significant tumor growth inhibition than IR or DOX, indicating that the combination of the two methods can enhance the efficacy of tumor killing (Figure 5). The enhanced anti-tumor effect was confirmed by histological analysis, revealing increased apoptosis in tumor xenografts in the mice treated with IR/DOX (Figure 6). From the above results, we suggest that the improved anti-tumor efficacy of the IR/DOX treatment may be associated with the decrease of SOD and CAT activity and the increase in ROS levels. On the one hand, when the tumor tissue is subjected to IR, many ROS are locally generated. On the other hand, many previous studies have demonstrated that the major mechanism of DOX-induced apoptosis is associated with excessive generation of intracellular ROS.[35,36] Therefore, these two methods can result in local high ROS concentrations and induce the apoptosis of tumor cells.

Conclusion

In this work, UTMD has temporarily blocked the perfusion of tumor tissue for approximately 1 hr. When IR happened, significantly decreased levels of both SOD and CAT activity

and increased levels of ROS were achieved, suggesting that UTMD induced IR participated in the generation of ROS, which in turn had an important role in the enhanced anti-tumor effect of DOX. Thus, our findings demonstrated that UTMD may be a novel, simple and non-invasive technique for IR of tumors, and its combination with chemotherapy may greatly improve anti-tumor efficacy.

Ethical Approval

All applicable national and institutional guidelines for the care and use of animals were followed. This article does not contain any studies with human participants performed by any of the authors.

Author Contributions

All authors contributed to data analysis, drafting or revising the article, gave final approval of the version to be published, and agree to be accountable for all aspects of the work.

Funding

This work was supported by the National Natural Science Foundation of China (Grant Nos. 81371559, 81671709, 81701711, 81871371), Science and Technology Program of Guangzhou (Grant No. 201804010106), Shenzhen Peacock Plan Tech. Inno. (KQJSCX20170331161449).

Disclosure

The authors report no conflicts of interest in this work.

References

1. Taratula O, Dani RK, Schumann C, et al. Multifunctional nanomedicine platform for concurrent delivery of chemotherapeutic drugs and mild hyperthermia to ovarian cancer cells. *Int J Pharm*. 2013;458(1):169–180. doi:10.1016/j.ijpharm.2013.09.032
2. He C, Liu D, Lin W. Self-assembled core-shell nanoparticles for combined chemotherapy and photodynamic therapy of resistant head and neck cancers. *ACS Nano*. 2015;9(1):991–1003. doi:10.1021/nn506963h
3. Wu H, Liu S, Gong J, et al. VCPA, a novel synthetic derivative of alpha-tocopheryl succinate, sensitizes human gastric cancer to doxorubicin-induced apoptosis via ROS-dependent mitochondrial dysfunction. *Cancer Lett*. 2017;393:22–32. doi:10.1016/j.canlet.2017.02.007
4. Nogueira V, Hay N. Molecular pathways: reactive oxygen species homeostasis in cancer cells and implications for cancer therapy. *Clin Cancer Res*. 2013;19(1078–0432(Print)):4309–4314. doi:10.1158/1078-0432.CCR-12-1424
5. Trachootham D, Alexandre J, Huang P. Targeting cancer cells by ROS-mediated mechanisms: a radical therapeutic approach? *Nat Rev Drug Discov*. 2009;8(7):579–591. doi:10.1038/nrd2803
6. Pelicano H, Feng L, Zhou Y, et al. Inhibition of mitochondrial respiration: a novel strategy to enhance drug-induced apoptosis in human leukemia cells by a reactive oxygen species-mediated mechanism. *J Biol Chem*. 2003;278(39):37832–37839. doi:10.1074/jbc.M301546200
7. Zhou Y, Hileman EO, Plunkett W, Keating MJ, Huang P. Free radical stress in chronic lymphocytic leukemia cells and its role in cellular sensitivity to ROS-generating anticancer agents. *Blood*. 2003;101(10):4098–4104. doi:10.1182/blood-2002-08-2512
8. Zhou JF, Chen P, Zhou YH, Zhang L, Chen HH. 3,4-Methylenedioxymethamphetamine (MDMA) abuse may cause oxidative stress and potential free radical damage. *Free Radic Res*. 2003;37(5):491–497. doi:10.1080/1071576031000076286
9. Fang J, Seki T, Maeda H. Therapeutic strategies by modulating oxygen stress in cancer and inflammation. *Adv Drug Deliv Rev*. 2009;61(4):290–302. doi:10.1016/j.addr.2009.02.005
10. Dixit D, Ghildiyal R, Anto NP, Sen E. Chaetocin-induced ROS-mediated apoptosis involves ATM-YAP1 axis and JNK-dependent inhibition of glucose metabolism. *Cell Death Dis*. 2014;5:e1212. doi:10.1038/cddis.2014.179
11. Hynynen K, Chung AH, Colucci V, Jolesz FA. Potential adverse effects of high-intensity focused ultrasound exposure on blood vessels in vivo. *Ultrasound Med Biol*. 1996;22(2):193–201. doi:10.1016/0301-5629(95)02044-6
12. Luo W, Wen G, Yang L, et al. Dual-targeted and pH-sensitive doxorubicin prodrug-microbubble complex with ultrasound for tumor treatment. *Theranostics*. 2017;7(2):452–465. doi:10.7150/thno.16677
13. Liu HL, Fan CH, Ting CY, Yeh CK. Combining microbubbles and ultrasound for drug delivery to brain tumors: current progress and overview. *Theranostics*. 2014;4(4):432–444. doi:10.7150/thno.8074
14. Chang EL, Ting CY, Hsu PH, et al. Angiogenesis-targeting microbubbles combined with ultrasound-mediated gene therapy in brain tumors. *J Control Release*. 2017;255:164–175. doi:10.1016/j.jconrel.2017.04.010
15. Maloney E, Khokhlova T, Pillarisetty VG, et al. Focused ultrasound for immuno-adjuvant treatment of pancreatic cancer: an emerging clinical paradigm in the era of personalized oncotherapy. *Int Rev Immunol*. 2017;36(6):338–351. doi:10.1080/08830185.2017.1363199
16. Ma R, Wu Q, Si T, Chang S, Xu RX. Oxygen and indocyanine green loaded microparticles for dual-mode imaging and sonodynamic treatment of cancer cells. *Ultrason Sonochem*. 2017;39:197–207. doi:10.1016/j.ultsonch.2017.03.019
17. Lentacker I, De Cock I, Deckers R, De Smedt SC, Moonen CT. Understanding ultrasound induced sonoporation: definitions and underlying mechanisms. *Adv Drug Deliv Rev*. 2014;72:49–64. doi:10.1016/j.addr.2013.11.008
18. Liu Z, Gao S, Zhao Y, et al. Disruption of tumor neovasculature by microbubble enhanced ultrasound: a potential new physical therapy of anti-angiogenesis. *Ultrasound Med Biol*. 2012;38(2):253–261. doi:10.1016/j.ultrasmedbio.2011.11.007
19. Gao Y, Gao S, Zhao B, et al. Vascular effects of microbubble-enhanced, pulsed, focused ultrasound on liver blood perfusion. *Ultrasound Med Biol*. 2012;38(1):91–98. doi:10.1016/j.ultrasmedbio.2011.09.018
20. Yan F, Li X, Jin Q, et al. Therapeutic ultrasonic microbubbles carrying paclitaxel and LyP-1 peptide: preparation, characterization and application to ultrasound-assisted chemotherapy in breast cancer cells. *Ultrasound Med Biol*. 2011;37(5):768–779. doi:10.1016/j.ultrasmedbio.2011.02.006
21. Carson AR, McTiernan CF, Lavery L, et al. Ultrasound-targeted microbubble destruction to deliver siRNA cancer therapy. *Cancer Res*. 2012;72(23):6191–6199. doi:10.1158/0008-5472.CAN-11-4079
22. Chen H, Hwang JH. Ultrasound-targeted microbubble destruction for chemotherapeutic drug delivery to solid tumors. *J Ther Ultrasound*. 2013;1:10. doi:10.1186/2050-5736-1-10
23. Tang HL, Wang ZG, Li Q, et al. Targeted delivery of bone mesenchymal stem cells by ultrasound destruction of microbubbles promotes kidney recovery in acute kidney injury. *Ultrasound Med Biol*. 2012;38(4):661–669. doi:10.1016/j.ultrasmedbio.2012.01.003
24. Chang S, Si T, Zhang S, Merrick MA, Cohn DE, Xu RX. Ultrasound mediated destruction of multifunctional microbubbles for image guided delivery of oxygen and drugs. *Ultrason Sonochem*. 2016;28:31–38. doi:10.1016/j.ultsonch.2015.06.024

25. Li P, Zhu M, Xu Y, et al. Impact of microbubble enhanced, pulsed, focused ultrasound on tumor circulation of subcutaneous VX2 cancer. *Chin Med J*. 2014;127(14):2605–2611.
26. Poillet-Perez L, Despouy G, Delage-Mourroux R, Boyer-Guittaut M. Interplay between ROS and autophagy in cancer cells, from tumor initiation to cancer therapy. *Redox Biol*. 2015;4:184–192. doi:10.1016/j.redox.2014.12.003
27. Xu Z, Jiang H, Zhu Y, et al. Cryptotanshinone induces ROS-dependent autophagy in multidrug-resistant colon cancer cells. *Chem Biol Interact*. 2017;273:48–55. doi:10.1016/j.cbi.2017.06.003
28. Wang J, Luo B, Li X, et al. Inhibition of cancer growth in vitro and in vivo by a novel ROS-modulating agent with ability to eliminate stem-like cancer cells. *Cell Death Dis*. 2017;8(6). doi:10.1038/cddis.2017.518
29. Pelicano H, Carney D, Huang P. ROS stress in cancer cells and therapeutic implications. *Drug Resist Updat*. 2004;7(2):97–110. doi:10.1016/j.drup.2004.01.004
30. Kong Q, Beel JA, Lillehei KO. A threshold concept for cancer therapy. *Med Hypotheses*. 2000;55(1):29–35. doi:10.1054/mehy.1999.0982
31. Park SY, Chang I, Kim JY, et al. Resistance of mitochondrial DNA-depleted cells against cell death: role of mitochondrial superoxide dismutase. *J Biol Chem*. 2004;279(9):7512–7520. doi:10.1074/jbc.M307677200
32. Hileman EO, Liu J, Albitar M, Keating MJ, Huang P. Intrinsic oxidative stress in cancer cells: a biochemical basis for therapeutic selectivity. *Cancer Chemother Pharmacol*. 2004;53(3):209–219. doi:10.1007/s00280-003-0726-5
33. Du H, Yang W, Chen L, et al. Emerging role of autophagy during ischemia-hypoxia and reperfusion in hepatocellular carcinoma. *Int J Oncol*. 2012;40(6):2049–2057. doi:10.3892/ijo.2012.1415
34. Song LL, Tu YY, Xia L, et al. Targeting catalase but not peroxiredoxins enhances arsenic trioxide-induced apoptosis in K562 cells. *PLoS One*. 2014;9(8):e104985. doi:10.1371/journal.pone.0104985
35. Shokoohinia Y, Hosseinzadeh L, Moieni-Arya M, Mostafaie A, Mohammadi-Motlagh HR. Osthole attenuates doxorubicin-induced apoptosis in PC12 cells through inhibition of mitochondrial dysfunction and ROS production. *Biomed Res Int*. 2014;2014:156848. doi:10.1155/2014/156848
36. Wang Z, Wang J, Xie R, Liu R, Lu Y. Mitochondria-derived reactive oxygen species play an important role in Doxorubicin-induced platelet apoptosis. *Int J Mol Sci*. 2015;16(5):11087–11100. doi:10.3390/ijms160511087